Monthly Notices
of the
ROYAL ASTRONOMICAL SOCIETY

MNRAS **460,** 1033–1038 (2016)
Advance Access publication 2016 May 1

doi:10.1093/mnras/stw1036

A new investigation of the possible X-ray counterparts of the magnetar candidate AX J1845−0258

Fabio Pintore★ and Sandro Mereghetti
INAF – IASF Milano, Via E. Bassini 15, I-20133 Milano, Italy

Accepted 2016 April 28. Received 2016 April 28; in original form 2016 March 22

ABSTRACT

AX J1845−0258 is a transient X-ray pulsar, with spin period of 6.97 s, discovered with the *ASCA* satellite in 1993. Its soft spectrum and the possible association with a supernova remnant suggest that AX J1845−0258 might be a magnetar, but this has not been confirmed yet. A possible counterpart one order of magnitude fainter, AX J184453−025640, has been found in later X-ray observations, but no pulsations have been detected. In addition, some other X-ray sources are compatible with the pulsar location, which is in a crowded region of the Galactic plane. We have carried out a new investigation of all the X-ray sources in the *ASCA* error region of AX J1845−0258, using archival data obtained with *Chandra* in 2007 and 2010, and with *XMM–Newton* in 2010. We set an upper limit of 6 per cent on the pulsed fraction of AX J184453−025640 and confirmed its rather hard spectrum (power-law photon index of 1.2 ± 0.3). In addition to the other two fainter sources already reported in the literature, we found other X-ray sources positionally consistent with AX J1845−0258. Although many of them are possibly foreground stars likely unrelated to the pulsar, at least another new source, CXOU J184457.5−025823, could be a plausible counterpart of AX J1845−0258. It has a flux of 6×10^{-14} erg cm^{-2} s^{-1} and a spectrum well fitted by a power law with photon index ∼1.3 and $N_{\rm H} \sim 10^{22}$ cm^{-2}.

Key words: magnetic fields – stars: magnetars – stars: neutron – pulsars: individual: AX J1845−0258 – infrared: stars – X-rays: binaries.

1 INTRODUCTION

AX J1845−0258 is an X-ray pulsar, with spin period of 6.97 s, discovered in a periodicity search for the sources in the 1993 *ASCA* archive (Gotthelf & Vasisht 1998; Torii et al. 1998). Further *ASCA* observations in 1997 did not detect it, while a fainter source, AX J184453−025640, positionally consistent with the pulsar, was found in an *ASCA* observation of the Galactic Plane Survey carried out in 1999. An association between the two sources, which would imply a flux decrease of a factor of ∼10, could not be confirmed because no pulsations were found in AX J184453−025640 (Vasisht et al. 2000). AX J184453−025640 is located at the centre of the radio-shell supernova remnant (SNR) G29.6+0.1 (Gaensler, Gotthelf & Vasisht 1999). A source consistent in flux and position with AX J184453−025640 was also seen with the *BeppoSAX* satellite in 2001 (Israel et al. 2004).

Based on the value of its spin period, on the soft X-ray spectrum (a blackbody with temperature $kT \sim 0.6$ keV or a steep power law with photon index $\Gamma \sim 5$), and on the possible association with an SNR (if indeed AX J184453−025640 and the pulsar are the same source), it was suggested that AX J1845−0258 could belong to the class of anomalous X-ray pulsars. These sources, together with the soft gamma-ray repeaters which show similar properties, are generally believed to be isolated neutron stars powered by strong magnetic fields, i.e. magnetars (see e.g. Mereghetti 2008).

Tam et al. (2006) analysed seven *Chandra* observations taken between 2003 June and August, and found three X-ray sources inside the large (3 arcmin radius) error box of AX J1845−0258 reported in Gotthelf & Vasisht (1998), the brightest one coinciding with AX J184453−025640. Its high absorption ($N_{\rm H} > 10^{22}$ cm^{-2}) was consistent with that of the pulsar seen in 1993, but again no pulsations could be detected. The other two *Chandra* sources were too faint for a detailed spectral and timing analysis.

These results indicate that AX J1845−0258 might be a transient magnetar, which experienced an outburst shortly before the 1993 *ASCA* observation and subsequently faded to quiescence. Similar behaviours are not unusual in magnetars (see e.g. Rea & Esposito 2011).

Here we present a new investigation of all the X-ray sources in the sky region of AX J1845−0258, based on *XMM–Newton* and *Chandra* archival data. These observations allowed us to carry out a more detailed spectral and timing analysis of the sources already

★ E-mail: pintore@iasf-milano.inaf.it

Table 1. Log of the *XMM–Newton* and *Chandra* observations.

Satellite	Obs.ID.	Observation date	Exposure (ks)
Chandra	7578	2007-02-19	4.7
Chandra	7579	2007-04-22	5.0
Chandra	7580	2007-06-08	4.8
Chandra	7581	2007-08-04	5.2
Chandra	7582	2007-09-18	5.1
Chandra	7583	2007-11-05	5.2
Chandra	11801	2010-06-17	32
XMM–Newton	0602350101	2010-04-14	61
XMM–Newton	0602350201	2010-04-16	43

reported in the literature and to discover other possible counterparts of AX J1845−0258.

2 OBSERVATIONS AND DATA REDUCTION

We used two *XMM–Newton* observations, with durations of 61 and 43 ks, carried out in 2010 April (see details in Table 1). The three cameras of the EPIC instrument (one pn camera; Strüder et al. 2001) and two MOS cameras (Turner et al. 2001) were operated in full-frame mode in both observations. The corresponding EPIC-pn and MOS read-out time resolution is 0.073 and 2.6 s, respectively. The data were reduced with SAS v. 14.0.0. We selected single- and double-pixel events (PATTERN $\leq$ 4) for the pn and single- and multiple-pixel events for the MOS (PATTERN $\leq$ 12). Time intervals with high particle background were excluded from the analysis, resulting in a net exposure time of $\sim$ 40 and $\sim$ 32 ks for the first and the second observation, respectively. We excluded from this work the 2003 *XMM–Newton* observation (Obs.ID: 0046540201) because it is affected by high particle background which limits the net exposure time to a few ks.

The seven *Chandra* observations used in this work were performed in 2007 and 2010, for a total exposure time of $\sim$ 60 ks (see Table 1). They were made using the ACIS-S detector in full-frame mode, yielding a time resolution of 3.241 s. We reduced the data with the CIAO software v.4.7 and the CALDB v.4.6.9.

For *XMM–Newton* data, we extracted the source counts from circular regions with radius 20 arcsec (except in a few cases mentioned below) and the background counts from nearby source-free circular regions with 40 arcsec radius. For *Chandra* data, we instead used circular regions with radius of 5 and 20 arcsec for source and background, respectively. Spectral fits were carried out with XSPEC v.12.8.2 in the energy range 0.3–10 keV. In the following, all the errors on the spectral parameters are at the 90 per cent c.l. For the timing analysis, the times of arrival of the counts were converted to the Solar system barycentre using the JPL planetary ephemerides DE405 and the *Chandra* coordinates of the sources.

3 DATA ANALYSIS AND RESULTS

We first created a combined EPIC image in the energy range 0.3–10 keV by stacking the pn and MOS data of both observations (Fig. 1, left). In addition to the three *Chandra* sources reported in Tam et al. (2006, labelled here as source F, O, and R), the EPIC data reveal the presence of seven new sources inside (or slightly outside) the error regions of AX J1845−0258. All of them are detected at $\geq 3\sigma$ in at least one of the considered energy ranges (0.3–10, 0.3–2, and 2–10 keV). The brightest of the new sources (*H* and *I*) are positionally coincident with the region of diffuse X-ray emission detected by Vasisht et al. (2000) in the *ASCA*-SIS data, which had a spatial resolution insufficient to resolve them.

We created a combined image in the 0.3–10 keV energy range by joining the data of the seven *Chandra* observations (Fig. 1, right). This image shows all the sources detected by *XMM–Newton* (except for source Q) plus 10 fainter ones. We note that 2003 *Chandra*

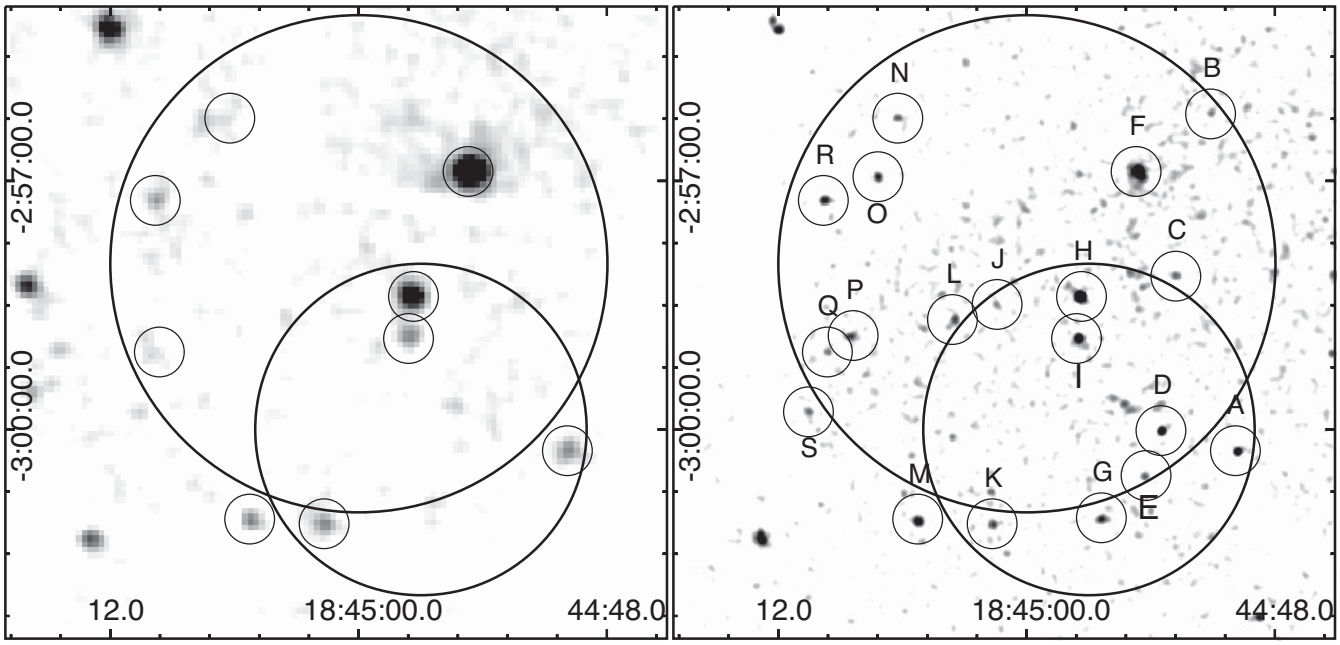

Figure 1. Left: EPIC image in the 0.3–10 keV energy range, obtained by stacking the pn and MOS data of the two *XMM–Newton* observations. The largest circle (3 arcmin radius) is the error region of AX J1845−0258 reported by Gotthelf & Vasisht (1998), while the smaller one (2 arcmin radius) is that reported by Torii et al. (1998). Right: stacking of all the 2007 and 2010 *Chandra* observations in the 0.3–10 keV energy range. In both images, the small circles (18 arcsec for graphical purposes only) indicate the sources found in this work. A smoothing has been applied to both images for display purposes.

Table 2. Summary of the X-ray sources detected in the *XMM–Newton* and *Chandra* observations.

Source	Name	RA	Dec.	Band[b]	Rate (*Chandra*)[c]	Rate (*XMM*/EPIC-pn)[c]	Other information[d]
A	CXOU J184449.8−030015	$18^h44^m49\overset{s}{.}8$	$-3°00'15\overset{''}{.}4$	S	$(7.1 \pm 1.4) \times 10^{-4}$	$(4.2 \pm 0.6) \times 10^{-3}$	$J = 14.30$, $K = 13.06$; late-type star
B	CXOU J184451.1−025611	$18^h44^m51\overset{s}{.}1$	$-2°56'11\overset{''}{.}5$	S	$(2.3 \pm 0.7) \times 10^{-4}$	–	$J = 8.96$, $K = 8.63$; late-type star
C	CXOU J184452.8−025809	$18^h44^m52\overset{s}{.}8$	$-2°58'09\overset{''}{.}0$	T	$(2.0 \pm 0.7) \times 10^{-4}$	–	$R1 = 17.97$, $I = 16.29$; star(?)
D	CXOU J184453.5−030000	$18^h44^m53\overset{s}{.}5$	$-3°00'00\overset{''}{.}8$	T	$(6.6 \pm 1.3) \times 10^{-4}$	–	$J = 12.96$, $K = 11.63$; late-type star
E	CXOU J184454.3−030033	$18^h44^m54\overset{s}{.}3$	$-3°00'33\overset{''}{.}3$	T	$(4.3 \pm 1.2) \times 10^{-4}$	–	$J = 15.31$, $K = 14.31$; late-type star
F	AX J184453−025640[a]	$18^h44^m54\overset{s}{.}7$	$-2°56'53\overset{''}{.}2$	H	$(4.8 \pm 0.3) \times 10^{-3}$	$(2.34 \pm 0.09) \times 10^{-2}$	
G	CXOU J184456.4−030104	$18^h44^m56\overset{s}{.}4$	$-3°01'04\overset{''}{.}6$	S	$(4.0 \pm 1.0) \times 10^{-4}$	–	$J = 13.41$, $K = 13.07$; star(?)
H	CXOU J184457.5−025823	$18^h44^m57\overset{s}{.}5$	$-2°58'23\overset{''}{.}7$	T	$(2.2 \pm 0.2) \times 10^{-3}$	$(1.1 \pm 0.1) \times 10^{-2}$	
I	CXOU J184457.6−025854	$18^h44^m57\overset{s}{.}6$	$-2°58'54\overset{''}{.}6$	S	$(7.3 \pm 1.2) \times 10^{-4}$	$(1.9 \pm 0.4) \times 10^{-3}$	$J = 10.27$, $K = 9.31$; late-type star
J	CXOU J184501.5−025829	$18^h45^m01\overset{s}{.}5$	$-2°58'29\overset{''}{.}5$	S	$(1.5 \pm 0.6) \times 10^{-4}$	–	
K	CXOU J184501.7−030108	$18^h45^m01\overset{s}{.}7$	$-3°01'08\overset{''}{.}2$	T	$(3.9 \pm 1.1) \times 10^{-4}$	$(3.1 \pm 0.5) \times 10^{-3}$	$J = 14.75$, $K = 11.95$; late-type star
L	CXOU J184503.8−025845	$18^h45^m03\overset{s}{.}8$	$-2°58'45\overset{''}{.}6$	S	$(1.6 \pm 0.6) \times 10^{-4}$	–	$J = 13.01$, $K = 12.28$; late-type star
M	CXOU J184505.3−030105	$18^h45^m05\overset{s}{.}3$	$-3°01'05\overset{''}{.}4$	T	$(7.9 \pm 1.5) \times 10^{-4}$	$(3.6 \pm 0.7) \times 10^{-3}$	$J = 13.77$, $K = 13.08$; late-type star
N	CXOU J184506.3−025614	$18^h45^m06\overset{s}{.}3$	$-2°56'14\overset{''}{.}6$	T	$(3.7 \pm 1.3) \times 10^{-4}$	$(2.0 \pm 0.4) \times 10^{-3}$	$J = 15.29$, $K = 12.80$; late-type star
O	CXOU J184507.2−025657[a]	$18^h45^m07\overset{s}{.}2$	$-2°56'57\overset{''}{.}4$	S	$(6.4 \pm 1.6) \times 10^{-4}$	–	$J = 13.73$, $K = 12.71$; late-type star
P	CXOU J184508.5−025852	$18^h45^m08\overset{s}{.}5$	$-2°58'52\overset{''}{.}0$	T	$(5.1 \pm 1.3) \times 10^{-4}$	–	$J = 16.01$, $K = 11.72$; late-type star
Q	CXOU J184509.7−025903	$18^h45^m09\overset{s}{.}7$	$-2°59'03\overset{''}{.}9$	H	–	$(1.8 \pm 0.4) \times 10^{-3}$	
R	CXOU J184509.8−025714[a]	$18^h45^m09\overset{s}{.}8$	$-2°57'14\overset{''}{.}1$	H	$(8.5 \pm 2.1) \times 10^{-4}$	$(1.2 \pm 0.4) \times 10^{-3}$	
S	CXOU J184510.6−025948	$18^h45^m10\overset{s}{.}6$	$-2°59'48\overset{''}{.}3$	S	$(2.4 \pm 0.8) \times 10^{-4}$	–	$J = 15.79$, $K = 13.39$; late-type star

Notes. [a]Also reported in Tam et al. (2006).
[b]Detection band: T: 0.3–10 keV; S: 0.3–2 keV; H: 2–10 keV.
[c]Count rate in the given detection band.
[d]Magnitude in J and K IR bands from the 2MASS catalogue, or $R1$ and I optical bands from the USNO B1 catalogue.

observations covered with high sensitivity only a small fraction of the pulsar error region; this explains why most of these sources were not reported by Tam et al. (2006).

We also looked in the optical USNO B1.0 (Monet et al. 2003) and infrared (IR) 2MASS (Skrutskie et al. 2006) catalogues for any possible counterpart of all the detected sources. The coordinates, count rates, and possible counterparts of the sources are listed in Table 2.

3.1 AX J184453−025640 (source F)

AX J184453−025640 is the brightest source presented in Tam et al. (2006). For the spectral analysis of this source, we first considered the two *XMM–Newton* observations separately. By fitting simultaneously the pn and MOS spectra with simple models (power law, blackbody), we obtained acceptable fits and found no evidence for time variations in the flux or spectral parameters. Therefore, also considering the short time interval between the two observations, we joined them and extracted a single spectrum combining pn+MOS data using the SAS tool EPICSPECCOMBINE. This allowed us to collect a total of ~ 2300 net counts in the 0.3–10 keV energy band.

In the individual observations, both a power law (photon index $\Gamma \sim 1$) and a blackbody (temperature in the range 2.1–2.4 keV) gave equally acceptable fits. However, the fit to the combined spectrum rebinned with a minimum of 200 counts per bin favours the power-law model (see Fig. 2 and Table 3).

The source count rates measured in the single *Chandra* observations were consistent with a constant, indicating no significant flux variability. Hence, for the *Chandra* spectral analysis, we created a stacked spectrum using all the observations and fitted it with a power law, fixing $N_{\rm H}$ to the value found with *XMM–Newton*. The resulting photon index (0.9 ± 0.5) and absorbed flux [$(3.3 \pm 0.75) \times 10^{-13}$ erg cm^{-2} s^{-1}, 2–10 keV] are consistent with those found with *XMM–Newton*.

In order to search for pulsations in AX J184453−025640, we used the EPIC-pn and MOS source counts of the two observations. We used only the counts with energy above 2 keV, where the signal-to-noise ratio is the highest. This yielded a total of about 1700 counts, of which ~ 16 per cent can be attributed to the background. Using a Rayleigh test technique, we explored periods in the range 6.5–7.5 s, which accounts for a possible spin-up or spin-down of the source of $|\dot{P}| < 10^{-9}$ s s^{-1} from 1993 up to the present days. No significant pulsations were detected and, by means of Monte Carlo simulations assuming a sinusoidal pulse profile, we could set a 3σ c.l. upper limit of 6 per cent on the source pulsed fraction (defined as the amplitude of the sinusoid divided by its average value).

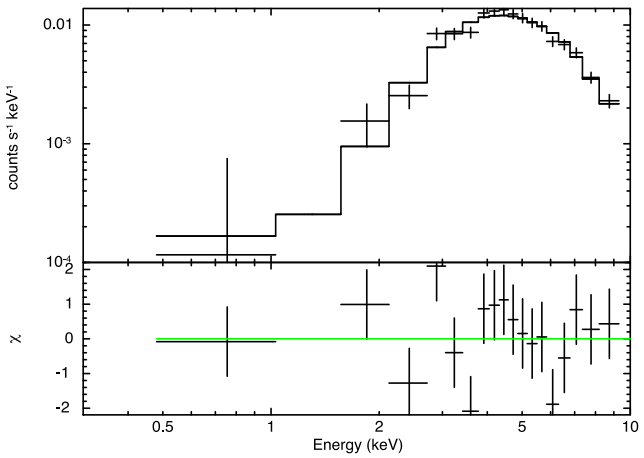

Figure 2. EPIC spectrum of AX J184453−025640 (source F). Top panel: data and best-fitting power-law model. Bottom panel: residuals in units of σ.

3.2 CXOU J184507.2−025657 (source O)

This source was first reported by Tam et al. (2006), who noted its positional coincidence with a near-IR object with magnitude $K = 12.7$ of the 2MASS catalogue. In *XMM–Newton*, we could not study it in detail since it fell very close to the gap between CCDs in the EPIC-pn data. In the *Chandra* observations, the source is

Table 3. EPIC spectral results. Errors are at 90 per cent for each parameter of interest.

Name	Source	Model	$N_{\rm H}$ (10^{22} cm^{-2})	Γ	$kT_{\rm bb}/kT_{\rm APEC}$ (keV)	Flux[a] (10^{-13} erg cm^2 s^{-1})	χ^2/dof
AX J184453−025640	F	POWERLAW	$9.7^{+2}_{-1.7}$	1.2 ± 0.3	–	3.1 ± 0.2	23.10/16 (0.11[b])
		BBODY	$5.8^{+1.3}_{-1.1}$	–	$2.1^{+0.3}_{-0.2}$	2.9 ± 0.2	27.12/16 (0.04[b])
CXOU J184457.5−025823	H	POWERLAW	$0.8^{+0.4}_{-0.3}$	1.3 ± 0.3	–	0.57 ± 0.07	8.06/9
		BBODY	$0.14^{+0.16}_{-0.12}$	–	$1.2^{+0.1}_{-0.1}$	$0.45^{+0.05}_{-0.06}$	8.95/9
CXOU J184457.6−025854	I	POWERLAW	$0.72^{+0.32}_{-0.65}$	$4.8^{+1.7}_{-3.8}$	–	$0.041^{+0.018}_{-0.012}$	17.24/11
		BBODY	$0.2^{+0.2}_{-0.5}$	–	$0.26^{+0.12}_{-0.13}$	$0.036^{+0.009}_{-0.011}$	18.81/11
		APEC	$0.75^{+0.19}_{-0.29}$	–	0.8 ± 0.2	0.042 ± 0.008	6.08/11
CXOU J184509.8−025714	R	POWERLAW		$0.9^{+1.5}_{-0.1}$	–	$0.22^{+0.09}_{-0.08}$	1.14/2
		BBODY		–	$1.5^{+1.0}_{-0.4}$	$0.18^{+0.09}_{-0.06}$	1.04/2

Notes.[a]Absorbed flux in the 0.3–10 keV energy band.
[b]Null hypothesis probability.
[c]Fixed.

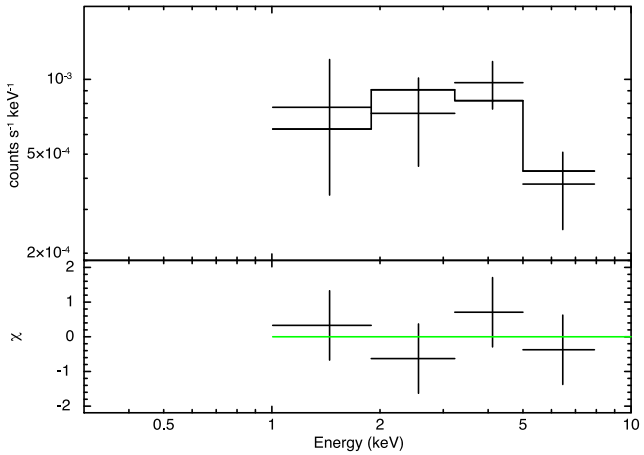

Figure 3. EPIC spectrum of source R stacking the spectra of the first and second *XMM–Newton* observations. Top panel: data and the best-fitting power-law model. Bottom panel: residuals in units of σ.

detected only in the soft energy band (0.3–2 keV). This finding and the association with a bright IR object suggest that this source is most likely a late-type star.

3.3 CXOU J184509.8−025714 (source R)

This was the faintest of the three *Chandra* sources previously reported by Tam et al. (2006). Due to its faintness, we could perform only a rough spectral analysis using the stacked EPIC spectrum of the two *XMM–Newton* observations, yielding about 180 spectral net counts in the 0.3–10 keV energy band. The source is hard and most of its photons are above 1.5 keV, making the estimates of the absorption poorly constrained. Therefore, we fixed the absorption at the value $N_{\rm H} = 1.69 \times 10^{22}$ cm^{-2}, corresponding to the total column density in the direction of the source (Dickey & Lockman 1990). We then fitted the spectrum with an absorbed power-law or a blackbody model. We found statistically acceptable results with both models (Table 3). Adopting the power-law model (Fig. 3), we estimated a source absorbed flux of $(2.2 \pm 0.9) \times 10^{-14}$ erg cm^{-2} s^{-1} in the energy range 0.3–10 keV. The spectrum of this source appears harder than expected for a magnetar in quiescence.

3.4 CXOU J184457.5−025823 (source H)

This source, reported here for the first time, is the second brightest object inside the error box of AX J1845−0258, only a factor of $\sim$ 2–3 fainter than AX J184453−025640. To avoid contamination from source I, we used an extraction radius of 15 arcsec. Since no evidence of variability was seen by comparing the spectra of the two *XMM–Newton* observations, we summed the pn and MOS spectra of the two observations, obtaining a total of 755 net counts in the 0.3–10 keV energy band.

The resulting spectrum, rebinned with a minimum of 100 counts per bin, was well fitted by either a blackbody with $kT = 1.2 \pm 0.1$ keV or by a power law with $\Gamma = 1.3 \pm 0.3$ (Table 3), while a thermal plasma model (APEC in XSPEC) gave a bad fit. From the power-law best fit (Fig. 4, left), we measured an absorbed flux of $(5.7 \pm 0.7) \times 10^{-14}$ erg cm^{-2} s^{-1}, in the 0.3–10 keV energy range.

Due to the limited counting statistics of the *Chandra* data, we extracted a spectrum by summing the counts of all the observations and fitted it with a power law keeping the column density fixed at the value $N_{\rm H} = 8 \times 10^{21}$ cm^{-2} derived with *XMM–Newton*. This yielded a photon index $\Gamma = 1.1 \pm 0.8$ and an absorbed flux of $(7.4 \pm 5) \times 10^{-14}$ erg cm^{-2} s^{-1} in the 0.3–10 keV range, implying that the source remained quite stable between 2007 and 2010.

We carried out a search for pulsations in source H, with the same procedure described above for AX J184453−025640 but, in this case, using the counts in the 1–12 keV energy range. Again no significant signals were found and we derived a 3σ c.l. upper limit of 18 per cent on the source pulsed fraction for periods in the range 6.5–7.5 s.

Finally, we remark that we could not associate any optical or IR counterpart to the source (see Fig. 5).

3.5 CXOU J184457.6−025854 (source I)

This source was too faint for a spectral analysis of the individual *XMM–Newton* observations. We extracted, from a region of 15 arcsec radius, a total pn+MOS source spectrum by summing the two *XMM–Newton* observations which gave us a total of 220 net counts in the 0.3–10 keV energy band. The fits with either a power law or a blackbody were acceptable but left several residuals ($\chi^2_\nu > 1.5$), while a good fit could be obtained with the APEC model (Fig. 4, right and Table 3). This gave a plasma temperature of 0.8 keV and an absorbed 0.3–10 keV flux of $(4.2 \pm 0.8) \times 10^{-15}$ erg cm^{-2} s^{-1}.

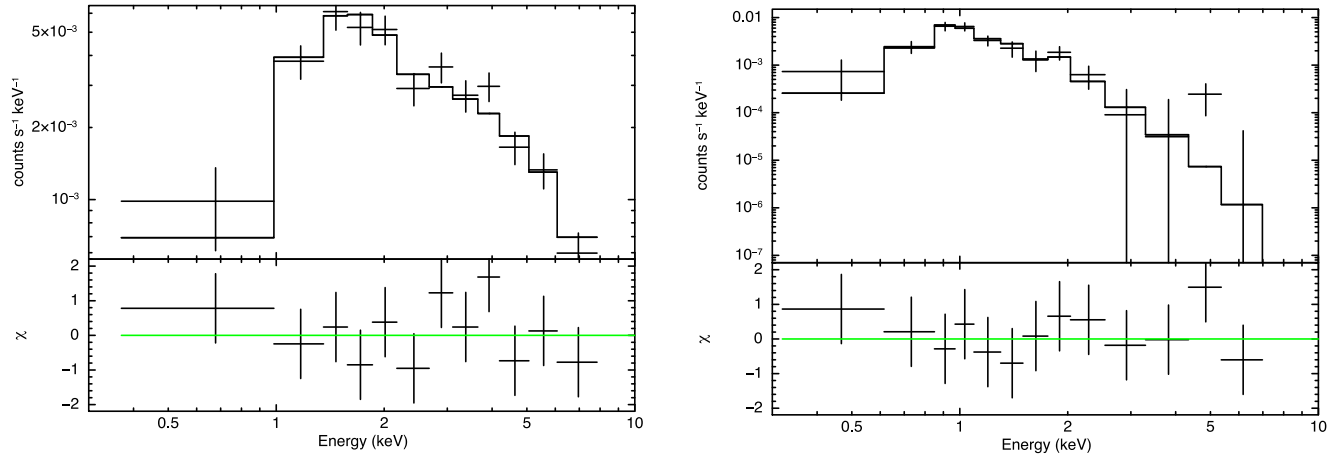

Figure 4. EPIC spectrum of sources H (left) and I (right) stacking the spectra of the first and second *XMM–Newton* observations. Top panels: data and the best-fitting power-law (left) and APEC (right) models. Bottom panels: residuals in units of σ.

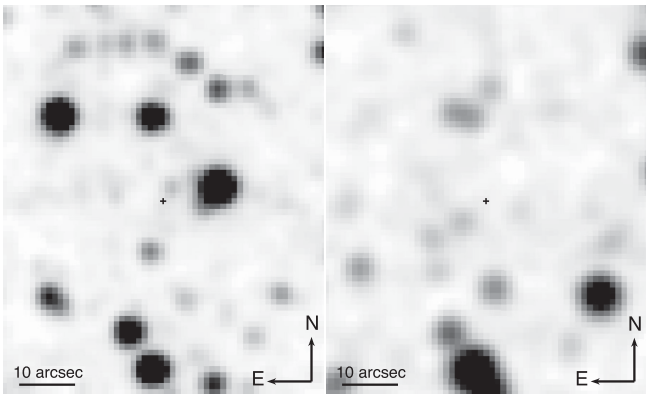

Figure 5. 2MASS *K*-band image (left) and DSS blue band (right) image of the field around source H. The cross is the source position with an uncertainty of 1 arcsec.

This source was too faint for a spectral analysis with the *Chandra* data.

Source I can be associated with an IR counterpart in 2MASS with magnitudes $J = 10.267 \pm 0.023$, $H = 9.542 \pm 0.025$, and $K = 9.305 \pm 0.025$. An optical counterpart can also be found with a $B1$-band magnitude of 15.29 ± 1. Based on the optical/IR colours and the thermal X-ray spectrum, we conclude that this object is most likely a foreground star of spectral type K or M.

3.6 CXOU J184505.3−030105 (source M)

Source M, positionally coincident with a 2MASS object with magnitudes of $J = 13.8$, $H = 12.6$, and $K = 13.1$, can be likely associated with a foreground late-type star. Its combined (pn+MOS of both observations) X-ray spectrum (218 net counts in the 0.3–10 keV band) is poorly constrained but can be well modelled ($\chi^2_\nu < 1$) with an APEC component. The best-fitting parameters are $N_{\rm H} = (5.7^{+6}_{-3}) \times 10^{22}$ cm^{-2}, $kT = 1.9^{+4}_{-1}$ keV, and a 0.3–10 keV absorbed flux of $(1.6 \pm 0.5) \times 10^{-14}$ erg cm^{-2} s^{-1}

3.7 CXOU J184501.7−030108 (source K)

Also source K can be associated with an IR source of the 2MASS catalogue with magnitudes in the *J*, *H*, and *K* bands of 14.745 ± 0.057, 12.779 ± 0.042, and 11.947 ± 0.035, respectively. No counterparts are reported in optical catalogues. The two *XMM–Newton* observations yielded ~ 300 net counts, and its X-ray spectrum can be well described with a single blackbody ($\chi^2/{\rm dof} = 7.09/7$) while a power-law or an APEC model is statistically worse. We found $N_{\rm H} < 1.5 \times 10^{21}$ cm^{-2}, $kT = 0.9^{+0.2}_{-0.1}$ keV, and a 0.3–10 keV absorbed flux of $(1.3 \pm 0.4) \times 10^{-14}$ erg cm^{-2} s^{-1}. Also in this case, a possible association with a foreground late-type star is likely.

3.8 CXOU J184449.8−030015 (source A)

Source A has an IR counterpart in the 2MASS catalogue with magnitudes in the *J*, *H*, and *K* bands of 14.296 ± 0.037, 13.472 ± 0.037, and 13.06 ± 1, respectively. An optical counterpart is also associated with the X-ray source, with magnitudes in the $R1$, $B1$, and *I* bands of 14.6 ± 1, 19.6 ± 1, and 15.25 ± 1, respectively. The combined source X-ray spectrum (~ 200 total net counts) could be well fitted with a blackbody or an APEC model. In the latter case, we found an $N_{\rm H} = (8^{+12}_{-6}) \times 10^{21}$ cm^{-2}, $kT = 3.8^{+3.7}_{-2.3}$ keV, and a 0.3–10 keV absorbed flux of $(1.2 \pm 0.6) \times 10^{-14}$ erg cm^{-2} s^{-1}. Because of its spectral properties and IR/optical emission, the source may be associated with a late-type star.

4 DISCUSSION AND CONCLUSIONS

After more than 20 years since its discovery, the nature of the pulsating X-ray source AX J1845−0258 is still unknown: it could be either a transient magnetar or a transient accreting X-ray binary containing a neutron star or a white dwarf. All the X-ray observations carried out after the 1993 discovery revealed only fainter sources, implying a variability of at least one order of magnitude, but none of them could be safely associated with AX J1845−0258 since the pulsations at 7 s were never detected again.

The brightest of these sources, AX J184453−025640, remains a good candidate for being the pulsar counterpart. The location at the centre of the SNR G29.6+0.1, the lack of a bright optical/IR counterpart, and the long-term light curve (see Fig. 6) strongly support the interpretation in terms of a transient magnetar. Our new upper limit on the pulsed fraction in AX J184453−025640 is incompatible with the strong modulation observed in AX J1845−0258. However, magnetars often show changes in their pulse profile when they evolve from an outburst towards quiescence, and some of them

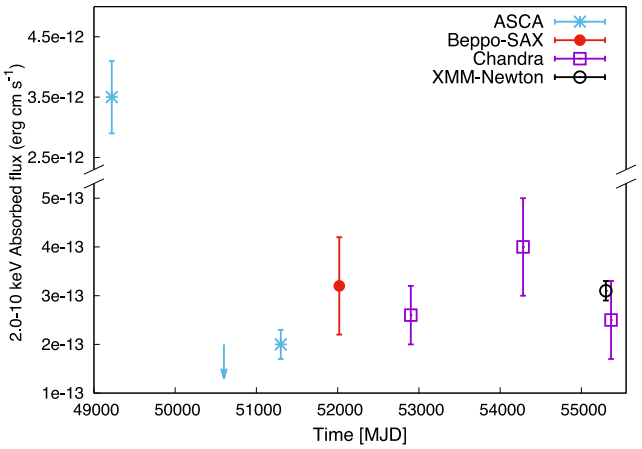

Figure 6. Absorbed 2–10 keV light curve of AX J184453−025640. The *ASCA*, *BeppoSAX,* and 2003 *Chandra* fluxes are taken from Tam et al. (2006). The *BeppoSAX* and *ASCA* fluxes might be overestimated due to the presence of other unresolved sources.

have pulsed fractions comparable with our upper limits (for example SGR 1806−20; e.g. Mereghetti et al. 2005 c; Woods et al. 2007). The nearly constant flux that the source has maintained for almost 16–17 years ($\sim 2.5 \times 10^{-13}$ erg cm^{-2} s^{-1}, Fig. 6) corresponds to an average luminosity of 3×10^{33} $(d/10\ \mathrm{kpc})^2$ erg s^{-1}, which is fully consistent with that of quiescent magnetars, while the relatively hard spectrum is the only characteristic of AX J184453−025640 that disfavours this interpretation. In fact, this spectrum is harder than that typically observed in magnetars, especially when they are in a quiescent state, and it is also harder than that measured for AX J1845−0258 in 1993.

Of course, it is also possible that AX J184453−025640 is a source totally unrelated to the pulsar. Its presence could have been easily missed in the 1993 *ASCA* data dominated by the much brighter X-ray pulsar. Besides AX J184453−025640, the *Chandra* and *XMM–Newton* data reported here show the presence of several faint X-ray sources. Many of them, with soft X-ray spectra and optical/IR counterparts, may be associated with foreground stars and are most likely not associated with AX J1845−0258. Only two of these sources were previously reported in the literature (CXOU J184507.2−025657 and CXOU J184509.8−025714; Tam et al. 2006). Amongst the other newly reported objects, we note that the sources H, J, and Q are not associated with any optical/IR counterpart.

Source H (CXOU J184457.5−025823), being the second brightest in the error region after AX J184453−025640, is particularly interesting. The lack of a bright optical/IR counterpart, together with a hard and highly absorbed spectrum, indicates that this source is unlikely to be a normal field star. On the other hand, its absorption is smaller than that of AX J184453−025640 (and of the pulsar seen in 1993) suggesting that source H is not a background AGN. Associating this source with the pulsar implies a variability of at least a factor of 60, still fully compatible with the variability seen in transient magnetars, but we note that source H lies outside the SNR.

We finally note that, although none of the X-ray sources reported here has optical/IR counterparts compatible with a high-mass X-ray binary, the possibility that AX J1845−0258 is a neutron star or white dwarf accreting from a low-mass companion cannot be excluded.

ACKNOWLEDGEMENTS

This work has been partially supported through financial contribution from the agreement ASI/INAF/I/037/12/0 and PRIN INAF 2014.

The results are in part based on observations obtained with *XMM–Newton*, an ESA science mission with instruments and contributions directly funded by ESA Member States and NASA, and on data obtained from the *Chandra* Data Archive. This publication makes partial use of data products from the Two Micron All Sky Survey, which is a joint project of the University of Massachusetts and the Infrared Processing and Analysis Center/California Institute of Technology, funded by the National Aeronautics and Space Administration and the National Science Foundation.

REFERENCES

Dickey J. M., Lockman F. J., 1990, ARA&A, 28, 215
Gaensler B. M., Gotthelf E. V., Vasisht G., 1999, ApJ, 526, L37
Gotthelf E. V., Vasisht G., 1998, New Astron., 3, 293
Israel G. et al., 2004, in Camilo F., Gaensler B. M., eds, Proc. IAU Symp. 218, Young Neutron Stars and Their Environments. Astron. Soc. Pac., San Francisco, p. 247
Mereghetti S., 2008, A&AR, 15, 225
Mereghetti S., Götz D., von Kienlin A., Rau A., Lichti G., Weidenspointner G., Jean P., 2005, ApJ, 624, L105
Monet D. G. et al., 2003, AJ, 125, 984
Rea N., Esposito P., 2011, in Torres D. F., Rea N., eds, Astrophysics and Space Science Proceedings, High-Energy Emission from Pulsars and Their Systems. Springer-Verlag, Berlin, p. 247
Skrutskie M. F. et al., 2006, AJ, 131, 1163
Strüder L. et al., 2001, A&A, 365, L18
Tam C. R., Kaspi V. M., Gaensler B. M., Gotthelf E. V., 2006, ApJ, 652, 548
Torii K., Kinugasa K., Katayama K., Tsunemi H., Yamauchi S., 1998, ApJ, 503, 843
Turner M. J. L. et al., 2001, A&A, 365, L27
Vasisht G., Gotthelf E. V., Torii K., Gaensler B. M., 2000, ApJ, 542, L49
Woods P. M., Kouveliotou C., Finger M. H., Göğüş E., Wilson C. A., Patel S. K., Hurley K., Swank J. H., 2007, ApJ, 654, 470

This paper has been typeset from a TEX/LATEX file prepared by the author.